# A Guided Self-Consistent-Field Method for Excited-State Wave Function Optimization: Applications to Ligand-Field Transitions in Transition-Metal Complexes

Bo Peng, Benjamin E. Van Kuiken, Feizhi Ding, and Xiaosong Li*

Department of Chemistry, University of Washington, Seattle, Washington 98195, United States

ABSTRACT: A guided self-consistent field (SCF) method is presented in this paper. This method uses the eigenspace update-and-following idea to improve the SCF method for optimizing wave functions that are higher-energy solutions to the Roothaan−Hall equation. In this method, the eigenvectors of the previous SCF step are used to prediagonalize the current Fock/Kohn−Sham matrix, preserving the ordering of orbital occupations. When the subject of interest is an excited state of the same spin symmetry as the ground state, the initial guess of excited wave function is improved with a preconditioning step. The preconditioning step is an SCF iteration applied to the β spin manifold if the initial guess is generated by orbital permutation in the α spin manifold. This simple preconditioning step gives rise to more-stable SCF convergence using the algorithm presented herein. The guided SCF method is used to optimize ligand-field excited states in tetrahedral transition-metal complexes, and calculate ΔSCF excitation energies. The calculated ligand-field transition energies are compared with those obtained from orbital energy differences, linear response time-dependent density functional theory, and experiments. The excitation energies obtained using the method presented in this work show a significant improvement over orbital energy differences and linear response method.
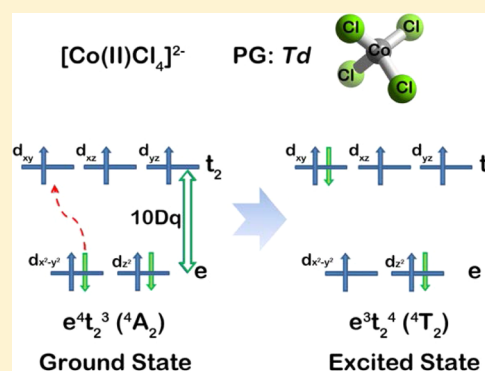
1. INTRODUCTION

Theoretical investigations of electronic excitations often require searching for excited-state wave functions while maintaining the orthogonality constraint. When wave function approximations (such as the finite basis approximation) are used, variational methods, such as the configurational interaction, can be used to obtain the upper bound of each excited state, fulfilling the bracketing theorem, $E_1 \leq \lambda_1 \leq E_2 \leq \lambda_2 ...$, where E and λ are, respectively, the exact and approximate solutions of excited states.[1] However, correlated electronic structure methods that satisfy both the orthogonality constraint and the bracketing theorem have prohibitive computational costs, except for systems with only a few electrons. Practical applications of excited-state calculations often use methods that avoid explicit computations of excited-state wave functions. For example, the linear response time-dependent density functional theory (LR-TDDFT) has been the workhorse for obtaining excitation energies at a very affordable computation cost.[2−9] LR-TDDFT computes the first-order response of ground-state electronic density to a small external perturbation. As a result, excitation energies are obtained as the resonant frequencies of the system. This approach is computationally inexpensive, because calculations of explicit excited-state wave functions are avoided.

In cases where excited-state wave functions are needed for analyzing molecular properties, the self-consistent field (SCF) method[10−15] can be used to obtain the approximate wave function of excited state. This method is based on the proof (under some assumptions) that there exist some higher-energy

solutions to the Roothaan−Hall equation (eq 1, presented later in this paper).[16,17] However, these solutions do not satisfy the bracketing theorem. As a result, they are just some stationary upper bounds of the ground state. Nevertheless, with careful scrutiny of the electronic characteristics of the higher-energy solutions, the electronic excitation energies can be approximated as the difference between the ground state and the SCF converged higher-energy states. When these two wave functions are associated with different spin manifolds (e.g., singlet and triplet), this technique is rather successful in predicting the spectra and electronic transition characteristics. When the excited state of interest has the same spin symmetry as the ground state (e.g., S_1 vs S_0), the excited state is approximated as a broken-spin-symmetry configuration state converged self-consistently to a higher-energy solution of the Roothaan−Hall equation. However, the approximate excited state often does not satisfy the orthogonality constraint. Although the lack of constraint of orthogonality to the ground state only leads to errors in the second-order term in the wave function,[18] it gives rise to convergence difficulty.[19] Conventional SCF techniques often lead to the variational collapse to the ground state, even if appropriate initial guesses of orbital occupations are used.

For electronic excitations of transition metals in ligand fields, standard ΔSCF often fails, because of small energy differences between SCF solutions and the high degeneracy of d-orbitals.

In such cases, one must include a constraint or guidance during the SCF procedure. Recently, controlled SCF methods using maximum overlap approach have been used to converge the SCF procedure to charge transfer and core excited states.[15,20] Inspired by the success of controlled SCF methods for optimizing excited-state wave functions, we proposed to use an eigenspace update-and-following method[21] to *guide* the SCF convergence to a higher-energy solution as an approximation to the excited state. The detailed discussion about the method and its robustness are presented in the Methodology section. In the Benchmark and Discussion section, we apply the guided SCF method to study ligand-field transitions in a select set of transition-metal complexes and compare these results with experimental values.

2. METHODOLOGY

Optimization of single particle wave functions as in HF and Kohn−Sham DFT can be achieved by iteratively solving the Roothaan−Hall equation in the atomic orbital (AO) basis:

$$\mathbf{FC} = \mathbf{SC}\epsilon \qquad (1)$$

where $\mathbf{F}$, $\mathbf{C}$, $\mathbf{S}$, and ϵ are the Fock/Kohn−Sham matrix, molecular orbital coefficients, overlap matrix, and orbital energy, respectively. For unrestricted HF and DFT, eq 1 is solved separately for α and β spins, with Fock/Kohn−Sham matrices constructed based on density matrices of both spins. In a conventional optimization of the ground-state wave function of an N-electron system, N number of spin orbitals $\{\varphi_i\}$ with the lowest energies are chosen to be occupied as an initial guess, while the rest of orbitals are unoccupied. The Slater determinant of such wave function can be specified by an occupation number vector, $|\mathbf{n}\rangle$, such as

$$|\mathbf{n}\rangle = |1_1, 1_2, ..., 1_N, 0_{N+1}, ..., 0_K\rangle \qquad (2)$$

where the subscript denotes the orbital and K is the basis size. Any permutation of occupation numbers between occupied and unoccupied orbitals results in an excited configuration state, which can be used as the initial guess for the excited-state wave function. In this work, we introduce a preconditioning step to the permuted initial guess when the subject of interest is an excited state of the same spin symmetry as the ground state (e.g., S_0 and S_1). Considering an initial guess for the excited-state wave function is generated by orbital permutation in the α spin manifold (e.g., $|\mathbf{n}\rangle_\alpha = |1_1, 1_2, ..., 0_N, 1_{N+1}, ..., 0_K\rangle_\alpha$) while the β spin remains in its ground-state configuration (e.g., $|\mathbf{n}\rangle_\beta = |1_1, 1_2, ..., 1_N, 0_{N+1}, ..., 0_K\rangle_\beta$). The preconditioning step is essentially an SCF iteration applied to the β manifold only. In this step, the Fock/Kohn−Sham matrix corresponding to the β spin is fully diagonalized while maintaining the α spin intact. The β spin wave function is reconstructed using the preconditioned eigenvectors of the β Fock/Kohn−Sham matrix. The purpose of this preconditioning step is obvious. It introduces a better Coulombic potential for optimization of the permuted spin-manifold, the α spin in this example. In our test cases, this simple preconditioning step gives rise to more-stable SCF convergence using the algorithm that is presented next.

In order to maintain the desired orbital occupation arrangement during the SCF procedure, we have implemented a guided-SCF method that combines prediagonalization step and eigenspace update techniques. The algorithm is constructed in an orthonormal basis. Transformation from AO (unprimed notation, e.g., $\mathbf{F}$ and $\mathbf{C}$) to orthonormal basis (primed notation, e.g., $\mathbf{F}'$ and $\mathbf{C}'$) can be achieved using the Löwdin method or the Cholesky method.[22−24] The details of this algorithm are presented in the following paragraphs.

In the ith SCF iteration, the Fock/Kohn−Sham matrix $\mathbf{F}'_i$ is formed using the occupied set of molecular orbitals (MOs) from the previous iteration $\mathbf{C}'_{i-1}$. Note that $\mathbf{C}'_0$ corresponds to the initial guess of excited configurational state. Although $\mathbf{C}'_i$ are not eigenvectors of $\mathbf{F}'_{i+1}$, they can be used to prediagonalize the Fock/Kohn−Sham matrix:

$$\Delta_{i+1} = \mathbf{C}'^\dagger_i \mathbf{F}'_{i+1} \mathbf{C}'_i \qquad (3)$$

The purpose of this intermediate prediagonalization step is to construct a diagonally dominant form of Fock/Kohn−Sham matrix. The transformed Fock/Kohn−Sham matrix is then diagonalized by a standard eigensolver yielding the eigenvalues and eigenvectors of the intermediate matrix:

$$\epsilon_{i+1} = \mathbf{A}^\dagger_{i+1} \Delta_{i+1} \mathbf{A}_{i+1} \qquad (4)$$

The eigenvectors of the Fock/Kohn−Sham matrix at the $(i+1)$th iteration are then computed using the following equation:

$$\mathbf{C}'_{i+1} = \mathbf{C}'_i \mathbf{A}_{i+1} \qquad (5)$$

In terms of computational cost, this approach is advantageous in most cases, since the diagonalization of a diagonal-dominant matrix (eq 4) is less expensive than direct diagonalization of a dense matrix, $\mathbf{F}'_i$. In the context of the guided SCF method developed here, the prediagonalization step is used to project the current Fock/Kohn−Sham matrix to the previous eigenvector space, preserving the ordering of orbital occupations. This step gives the guidance to the SCF procedure by maintaining the orbital occupations. In other words, instead of selecting the lowest-energy N number of spin−orbitals resulting from a direct diagonalization, the SCF proceeds by inheriting the orbital occupation arrangement from the previous step.

The guided SCF algorithm discussed above is implemented in the development version of the Gaussian program.[25] For all test cases, geometry optimizations were fully optimized with the T_d symmetry constraint. The metal d-orbitals are identified by population analysis and visual inspection. Initial excited configurational states are constructed by interchanging the occupation numbers of occupied and virtual orbitals, followed by wave function optimization using the guided SCF approach introduced here.

■ BENCHMARK AND DISCUSSION

One of the most important theories for understanding physical properties of transition-metal (TM) complexes is ligand-field theory. It has been successfully and widely used in the interpretation of optical, spin, and magnetic measurements of TM complexes. For ligand-field theory of octahedral and tetrahedral coordinations, the central parameter describing the metal−ligand environment is the ligand-field splitting energy, 10Dq, which can be readily observed in the $d−d$ spectra of TM complexes. Because of rather small excitation energies and high degeneracy of d-levels, ligand-field transitions are usually difficult to resolve. In this work, we apply the method introduced above to calculate ligand-field excitations in a select set of tetrahedral TM complexes.

The first test case is $[\mathrm{Co^{II}Cl_4}]^{2-}$ (Sec. 3), which has been the subject of extensive experimental and theoretical studies.[26−32] The tetrahedral ligand field splits d-levels into two d_e orbitals and three d_{t_2} orbitals ($\epsilon_e < \epsilon_{t_2}$). $[\mathrm{Co^{II}Cl_4}]^{2-}$ is a typical high-spin

complex with a $^4A_2$ ground state and an $e^4 t_2^3$ electron configuration. (See Figure 1.) The lowest spin-allowed $d-d$
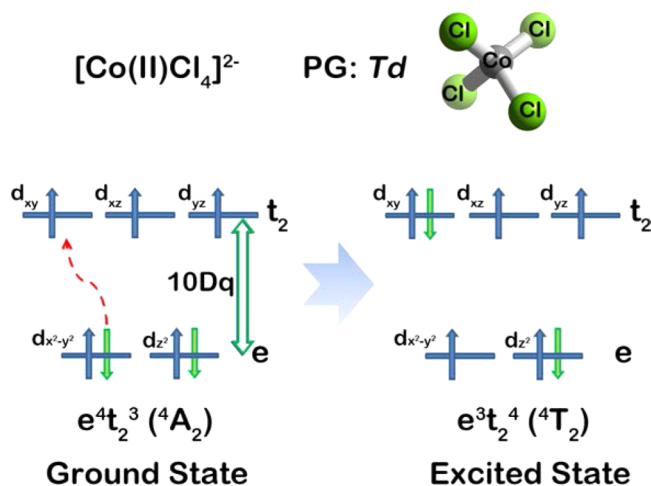

Figure 1. Schematic description of the electronic structure of the ground and excited states of $[Co^{II}Cl_4]^{2-}$ in the T_d ligand field.

transition corresponds to the $^4A_2 \rightarrow {}^4T_2(F)$ (Sec. 3) excitation. In order to obtain the energy and wave function of the $^4T_2$ state, the initial guess of the excited state is prepared by promoting an electron from the occupied $d_{x^2-y^2}$ to the unoccupied d_{xy} spin orbitals in the β manifold at the ground-state geometry (i.e., vertical excitation). Figure 2 shows the
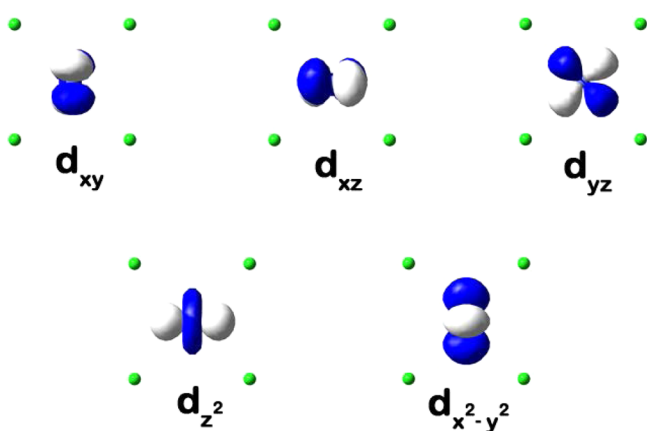

Figure 2. Frontier spin orbitals of $[Co^{II}Cl_4]^{2-}$ in the T_d ligand field.

Kohn–Sham orbitals whose populations are manipulated to generate the $d-d$ excited state. The guided SCF method is then used to optimize the wave function of the $^4T_2$ state. The energy difference between the fully optimized $^4T_2$ and $^4A_2$ states is the 10Dq value.

Table 1 compares experiments with the computed 10Dq values using the guided SCF method with various DFT functionals. We also include estimated 10Dq values using simple orbital energy differences, as well as those computed using the LR-TDDFT method. We have tested functionals at several different levels of approximation, including GGA (BLYP[33,34] and BP86), meta-GGA (TPSS[35]), hybrid GGA (B3LYP[36] and B97-2[37]), and meta hybrid GGA (TPSSh[38]) with pseudo-potential LANL2DZ,[39−41] and several full electron basis sets. The diversity of this test set is representative of the most commonly used DFT functionals for studies of ligand-

Table 1. Comparison of Ligand-Field Excitations in $[Co^{II}Cl_4]^{2-}$ ^{a}

	$\epsilon_{t_2} - \epsilon_e$ (eV)	LR-TDDFT (eV)	ΔSCF (eV)	
			$^4A_2 \rightarrow {}^4T_2(F)$	$^4A_2 \rightarrow {}^4T_1(F)$
B3LYP/LANL2DZ	0.04	0.64	0.32	0.91
BLYP/LANL2DZ	0.01	0.64	0.33	0.87
TPSS/LANL2DZ	0.01	0.65	0.34	1.00
TPSSh/LANL2DZ	0.07	0.65	0.33	1.02
B97−2/LANL2DZ	0.03	0.65	0.33	0.87
BP86/LANL2DZ	0.03	0.65	0.35	0.88
BP86/6-31+G(d)	0.05	0.73	0.40	1.00
BP86/cc-pVDZ	0.00	0.73	0.36	0.96
BP86/aug-cc-pVDZ	0.00	0.73	0.39	1.01

^{a}The experimental 10Dq ($^4A_2 \rightarrow {}^4T_2(F)$) value is ~0.39 eV.[31] Two-electron $d-d$ transition, $^4A_2 \rightarrow {}^4T_1(F)$, is observed at ~1 eV in Co^{2+}-doped ZnO.[43]

field excitations. These tests assess the consistency of each method for calculating ligand-field excitation energies. Table 1 shows that the t_2-e orbital energy difference (0.01−0.07 eV) severely underestimates the experimentally determined 10Dq value (~0.39 eV) as expected. On the other hand, the LR-TDDFT results overestimate the excitation energy by ~0.25 eV. The nature of the linear response theory describes one-electron excitation in the ground state electronic potential. It does not include wave function relaxation/optimization of the excited state. As a result, the LR-TDDFT method computes an upper bound of the excitation energy associated with local electronic transitions. Similar overestimation of $d-d$ transitions using LR-TDDFT has been reported for Co(III) and Rh(III) complexes.[42] In contrast, the ΔSCF results using the guided SCF method are in excellent agreement with the experimental 10Dq values.

In principle, the guided SCF technique for computing excited states and excitation energies is not restricted to single-electron excitation. We have also applied the guided SCF algorithm to calculate the wave function and excitation energy of the doubly excited state, $^4T_1(F)$. The procedure is similar to that for the $^4T_2(F)$ singly excited state. Beginning with the $^4T_2(F)$ singly excited state, a second β electron is promoted from the d_{z^2} orbital to an unoccupied orbital in the t_2 set, and this state is optimized. The excitation energy for the doubly excited state is given in Table 1. The ability of the guided SCF algorithm to isolate a state that is doubly excited with respect to the ground state reference, exhibits an advantage of ΔSCF techniques over LR-TDDFT from which double excitations cannot be obtained. The guided SCF method can be used as a computationally inexpensive approach for optimizing doubly excited electronic states.

Table 2 lists 10Dq values in various TM complexes in tetrahedral coordination computed at the BP86/LANL2DZ level of theory. The 10Dq values from the ΔSCF using the guided SCF method, LR-TDDFT, and experiment (where available) are compared. For all test cases, ΔSCF excitation energies are in very good agreement with the experiment. For most of the cases, the deviation of the guided SCF method result from the experimental value is <0.1 eV, whereas the linear response calculations overestimate the 10Dq values significantly.

Table 2. 10Dq Values Computed Using the Guided SCF Method for a Select Set of First-Row Transition-Metal Complexes at the BP86/LANL2DZ Level of Theory

	TM 3d configuration	spin multiplicity	LR-TDDFT (eV)	ΔE_1	exp	ref
				ΔSCF (eV)		
$[V(III)Cl_4]^-$	e^2	3	1.57	1.47	1.30	26
V(IV)Cl$_4$	e^1	2	1.57	1.02	1.12	26
Mn(IV)F$_4$	$e^2 t_2^1$	4	1.58	1.34	1.34	44
$[Fe(VI)O_4]^{2-}$	e^2	1	0.98	0.60	0.57	45
Fe(CO)$_4$	$e^3 t_2^3$	5	0.96	0.67		
$[Co(II)I_4]^{2-}$	$e^4 t_2^3$	4	0.60	0.30	0.33	26
Co(CO)$_4$	$e^4 t_2^3$	4	0.65	0.62		
$[Ni(VI)O_4]^{2-}$	$e^2 t_2^2$	5	0.60	0.77		
$[Ni(II)Cl_4]^{2-}$	$e^4 t_2^4$	3	0.75	0.35	0.51	26
$[Ni(II)(CN)_4]^{2-}$	$e^4 t_2^4$	3	0.78	0.45		
Ni(CO)$_4$	$e^4 t_2^4$	3	0.65	0.60		

3. CONCLUSION

In this paper, we introduced a guided self-consistent field (SCF) method for obtaining higher-energy solutions to the Roothaan−Hall equation as approximations to the excited states. This method uses the eigenspace update-and-following idea to maintain the orbital occupations chosen in the initial guess while allowing the wave function to be fully optimized. A preconditioning procedure is introduced to improve the initial guess generated using simple orbital permutation. This method has been applied to studies of ligand-field transitions in tetrahedral transition-metal (TM) complexes. The results were compared with experiments and other widely used methods. The ΔSCF excitation energies are in excellent agreement with experiments. This is a significant improvement over orbital energy differences and linear response time-dependent density functional theory (LR-TDDFT), which either significantly underestimate or overestimate excitation energies. Finally, the guided SCF algorithm provides a promising approach for optimizing multielectron excited states that cannot be accessed by other approaches.

■ APPENDIX: PROPERTIES OF THE EIGENVALUES AND EIGENVECTORS IN A NONLINEAR VARIATIONAL PROBLEM

Consider a reference N-electron Slater determinant Φ_0:

$$\Phi_0 = \hat{A} \prod_i \phi_i^0(i) \tag{6}$$

where $\hat{A}$ is the antisymmetrizer and ϕ_i^0 occupied spin orbitals of the reference state. Here, we label i, j, k, and l as occupied orbital indices, a, b, c, and d as unoccupied orbital indices, and p, q, r, and s as all orbital indices.

The SCF procedure can be recast in the formalism of orbital rotation as a unitary transformation of all of the spin orbitals:

$$\phi_p = \sum_q \phi_q^0 U_{qp} \tag{7}$$

Here, the unitary matrix $\mathbf{U}$ may be written in terms of an anti-Hermitian matrix $\mathbf{C}$:

$$\mathbf{U} = \exp(-\mathbf{C}) \tag{8}$$

where $\mathbf{C}^\dagger = -\mathbf{C}$. $\mathbf{C}$ is also called the orbital rotation matrix, and it satisfies

$$c_{ij} = c_{ab} = 0 \qquad \text{for all } i, j, a, b \tag{9}$$

It can be shown that the new Slater determinant that consists of the transformed orbitals can be expressed as

$$\Phi = \Phi_0 + \sum_{i,a} c_{ia}\Phi_i^a + \frac{1}{2}\sum_{i,a,j,b} c_{ia}c_{jb}\Phi_{ij}^{ab} + \cdots \tag{10}$$

where Φ_i^a, Φ_{ij}^{ab}, ... are the singly, doubly, ... excited determinants, with respect to the reference state Φ_0. Note that eq 10 is not the conventional CI-type expansion. It has constraints on the expansion coefficients as products of rotational matrix elements.

In the variational approach for the optimized determinant Φ, we consider the energy functional

$$E[\Phi] = \frac{\langle\Phi|\hat{H}|\Phi\rangle}{\langle\Phi|\Phi\rangle} \tag{11}$$

Substituting eq 10 into the above expression, we have

$$E(\mathbf{c}) = \frac{H_{00} + 2\mathbf{c}^\dagger\mathbf{S} + \mathbf{c}^\dagger\mathbf{Dc} + \cdots}{1 + \mathbf{c}^\dagger\mathbf{c} + \cdots} \tag{12}$$

where

$$H_{00} = \langle\Phi_0|\hat{H}|\Phi_0\rangle \tag{13}$$

$$S_I = \langle\Phi_0|\hat{H}|\Phi_I\rangle \tag{14}$$

$$D_{IJ} = \langle\Phi_I|\hat{H}|\Phi_J\rangle + \langle\Phi_0|\hat{H}|\Phi_{IJ}\rangle \tag{15}$$

The existence of higher-order terms in eq 12 indicates that the variation of $E(\mathbf{c})$ with respect to $\mathbf{c}$ is nonlinear. Mathematically, stationary points of eq 12 are usually characterized by their first- and second-order properties. If we truncate the energy functional up to second order in $\mathbf{c}$, eq 12 becomes

$$E(\mathbf{c}) \simeq \frac{H_{00} + 2\mathbf{c}^\dagger\mathbf{S} + \mathbf{c}^\dagger\mathbf{Dc}}{1 + \mathbf{c}^\dagger\mathbf{c}}$$

$$= \frac{(1 \quad \mathbf{c}^\dagger)\begin{pmatrix} H_{00} & \mathbf{S}^\dagger \\ \mathbf{S} & \mathbf{D} \end{pmatrix}\begin{pmatrix} 1 \\ \mathbf{c} \end{pmatrix}}{1 + \mathbf{c}^\dagger\mathbf{c}} \tag{16}$$

The stationary point of the truncated energy functional occurs when the gradient $\mathbf{g}$ vanishes:

$$\mathbf{g} = \frac{\partial E}{\partial \mathbf{c}} = \frac{2\begin{pmatrix} H_{00} & \mathbf{S}^\dagger \\ \mathbf{S} & \mathbf{D} \end{pmatrix}\begin{pmatrix} 1 \\ \mathbf{c} \end{pmatrix} - 2E\begin{pmatrix} 1 \\ \mathbf{c} \end{pmatrix}}{1 + \mathbf{c}^\dagger\mathbf{c}} = 0 \tag{17}$$

which leads to the usual eigenvalue problem,

$$\tilde{\mathbf{H}}\mathbf{x} = E\mathbf{x} \tag{18}$$

where

$$\tilde{\mathbf{H}} = \begin{pmatrix} H_{00} & \mathbf{S}^\dagger \\ \mathbf{S} & \mathbf{D} \end{pmatrix} \tag{19}$$

$$\mathbf{x} = \begin{pmatrix} 1 \\ \mathbf{c} \end{pmatrix} \tag{20}$$

Therefore, the solutions of the variational Schrödinger equation amounts to the stationary points of the energy functional which has $N + 1$ number of roots, where N is the dimension of $\mathbf{c}$.

The characteristics of these stationary points can be verified by evaluating the second derivatives, Hessian $\mathbf{h}$, given by

$$\mathbf{h} = \frac{\partial^2 E}{\partial \mathbf{c}^2} = -\frac{4(\tilde{\mathbf{H}}\mathbf{x} - E\mathbf{x})\mathbf{x}^\dagger}{(\mathbf{x}^\dagger \mathbf{x})^2} + \frac{2(\tilde{\mathbf{H}} - E\mathbf{I} + \mathbf{g}\mathbf{x}^\dagger)}{\mathbf{x}^\dagger \mathbf{x}} \tag{21}$$

where $\mathbf{I}$ is the identity matrix. In deriving eqs 17 and 21, we have applied the usual convention for matrix/vector differentiations.

At stationary points, the Hessian becomes

$$\mathbf{h}|_{\mathbf{g}=0} = \frac{2(\tilde{\mathbf{H}} - E\mathbf{I})}{\mathbf{x}^\dagger \mathbf{x}} \tag{22}$$

When expressed in the normalized eigenspace of the matrix $\tilde{\mathbf{H}}$, the Hessian becomes

$$\mathbf{h}'|_{\mathbf{g}=0} = \begin{pmatrix} E_0 - E & 0 & \cdots & 0 \\ 0 & E_1 - E & \cdots & 0 \\ \vdots & \vdots & \ddots & \vdots \\ 0 & \cdots & 0 & E_M - E \end{pmatrix} \tag{23}$$

where E_0 stands for the ground-state energy and E_i is the energy of the ith excited state.

It is easy to see that, at the ground state (i.e., when $E = E_0$), all the diagonal elements of the Hessian are non-negative, which implies a minimum, whereas at the ith excited state (i.e., when $E = E_i$), there are i negative diagonal elements in the Hessian, indicating an ith saddle point.

■ AUTHOR INFORMATION

Corresponding Author
*E-mail: li@chem.washington.edu.

Notes
The authors declare no competing financial interest.

■ ACKNOWLEDGMENTS

■ REFERENCES

(1) Lowdin, P. O. In *Proceedings of an Advanced Seminar on Perturbation Theory and Its Applications in Quantum Mechanics*; Wilcox, C. H., Ed.; Wiley: New York, 1966; pp 255−294.
(2) Gross, E. K. U.; Dobson, J. F.; Petersilka, M. In *Topics in Current Chemistry*; Nalewajski, R. F., Ed.; Springer−Verlag: Heidelberg, 1996; pp 81−172.
(3) Onida, G.; Reinig, L.; Rubio, A. *Rev. Mod. Phys.* **2002**, *74*, 601−659.
(4) Casida, M. E. In *Recent Advances in Density-Functional Methods*; Chong, D. A., Ed.; World Scientific: Singapore, 1995; pp 155−192.
(5) Casida, M. E. In *Theoretical and Computational Chemistry*; Seminario, J. M., Ed.; Elsevier: Amsterdam, 1996; pp 391−439.
(6) Stratmann, R. E.; Scuseria, G. E.; Frisch, M. J. *J. Chem. Phys.* **1998**, *109*, 8218−8224.
(7) Dreuw, A.; Head-Gordon, M. *Chem. Rev.* **2005**, *105*, 4009−4037.
(8) Casida, M. E. *J. Mol. Struct.: THEOCHEM* **2009**, *914*, 3−18.
(9) Liang, W.; Fischer, S. A.; Frisch, M. J.; Li, X. *J. Chem. Theor. Comput.* **2011**, *7*, 3540−3547.
(10) Gunnarsson, O.; Lundqvist, B. I. *Phys. Rev. B* **1976**, *13*, 4274−4298.
(11) Jones, R. O.; Gunnarsson, O. *Rev. Mod. Phys.* **1989**, *61*, 689−746.
(12) Hellman, A.; Razaznejad, B.; Lundqvist, B. I. *J. Chem. Phys.* **2004**, *120*, 4593−4602.
(13) Görling, A. *Phys. Rev. A* **1999**, *59*, 3359−3374.
(14) Behler, J.; Delley, B.; Reuter, K.; Scheffler, M. *Phys. Rev. B* **2007**, *75*, 115409−115418.
(15) Gilbert, A. T. B.; Besley, N. A.; Gill, P. M. W. *J. Phys. Chem. A* **2008**, *112*, 13164−13171.
(16) Lions, P. *Commun. Math. Phys.* **1987**, *109*, 33−97.
(17) Stanton, R. E. *J. Chem. Phys.* **1968**, *48*, 257−262.
(18) Helgaker, T.; Jørgensen, P.; Olsen, J. *Molecular Electronic Structure Theory*; John Wiley & Sons, Inc.: New York, 2000; pp 107−141.
(19) Young, D. C. *Computational Chemistry: A Practical Guide for Applying Techniques to Real-World Problems*; John Wiley & Sons, Inc.: New York, 2001.
(20) Besley, N. A.; Gilbert, A. T. B.; Gill, P. M. W. *J. Chem. Phys.* **2009**, *130*, 124308−124314.
(21) Liang, W.; Wang, H.; Hung, J.; Li, X.; Frisch, M. J. *J. Chem. Theor. Comput.* **2010**, *6*, 2034−2039.
(22) Millam, J. M.; Scuseria, G. E. *J. Chem. Phys.* **1997**, *106*, 5569−5577.
(23) Li, X.; Millam, J. M.; Scuseria, G. E.; Frisch, M. J.; Schlegel, H. B. *J. Chem. Phys.* **2003**, *119*, 7651.
(24) Li, X.; Moss, C. L.; Liang, W.; Feng, Y. *J. Chem. Phys.* **2009**, *130*, 234115.
(25) Frisch, M. J.; Trucks, G. W.; Schlegel, H. B.; Scuseria, G. E.; Robb, M. A.; Cheeseman, J. R.; Scalmani, G.; Barone, V.; Mennucci, B.; Petersson, G. A.; Nakatsuji, H.; Caricato, M.; Li, X.; Hratchian, H. P.; Izmaylov, A. F.; Bloino, J.; Zheng, G.; Sonnenberg, J. L.; Liang, W.; Hada, M.; Ehara, M.; Toyota, K.; Fukuda, R.; Hasegawa, J.; Ishida, M.; Nakajima, T.; Honda, Y.; Kitao, O.; Nakai, H.; Vreven, T.; J. A. Montgomery, J.; Peralta, J. E.; Ogliaro, F.; Bearpark, M.; Heyd, J. J.; Brothers, E.; Kudin, K. N.; Staroverov, V. N.; Keith, T.; Kobayashi, R.; Normand, J.; Raghavachari, K.; Rendell, A.; Burant, J. C.; Iyengar, S. S.; Tomasi, J.; Cossi, M.; Rega, N.; Millam, J. M.; Klene, M.; Knox, J. E.; Cross, J. B.; Bakken, V.; Adamo, C.; Jaramillo, J.; Gomperts, R.; Stratmann, R. E.; Yazyev, O.; Austin, A. J.; Cammi, R.; Pomelli, C.; Ochterski, J. W.; Martin, R. L.; Morokuma, K.; Zakrzewski, V. G.; Voth, G. A.; Salvador, P.; Dannenberg, J. J.; Dapprich, S.; Parandekar, P. V.; Mayhall, N. J.; Daniels, A. D.; Farkas, O.; Foresman, J. B.; Ortiz, J. V.; Cioslowski, J.; ; Fox, D. J. *Gaussian Development Version, Revision H.21*; Gaussian, Inc.: Wallingford, CT, 2012.
(26) Lever, A. B. P. *Inorganic Electronic Spectroscopy*; Elsevier: Amsterdam, 1984.
(27) Johansen, H.; Andersen, N. *Mol. Phys.* **1986**, *58*, 965−975.
(28) Hipps, K. W.; Mazur, U. *J. Am. Chem. Soc.* **1987**, *109*, 3861−3865.
(29) Soudackov, A. V.; Tchougreeff, A. L.; Misurkin, Y. A. *Theor. Chim. Acta* **1992**, *83*, 389−416.
(30) Cassam-Chenai, P.; Wolff, S. K.; Chandler, G. S.; Figgis, B. N. *Int. J. Quantum Chem.* **1996**, *60*, 667−680.
(31) Nover, J.; Schmidtke, H. H. *Chem. Phys.* **1999**, *241*, 179−191.
(32) Maestre, J. M.; Lopez, X.; Bo, C.; Poblet, J. M. *Inorg. Chem.* **2002**, *41*, 1883−1888.
(33) Becke, A. D. *Phys. Rev. A* **1988**, *38*, 3098−3100.
(34) Lee, C.; Yang, W.; Parr, R. G. *Phys. Rev. B* **1988**, *37*, 785−789.
(35) Tao, J.; Perdew, J. P.; Staroverov, V. N.; Scuseria, G. E. *Phys. Rev. Lett.* **2003**, *91*, 146401.

(36) Stephens, P. J.; Devlin, F. J.; Chabalowski, C. F.; Frisch, M. J. *J. Phys. Chem.* **1994**, *98*, 11623−11627.

(37) Wilson, P. J.; Bradley, T. J.; Tozer, D. J. *J. Chem. Phys.* **2001**, *115*, 9233−9242.

(38) Staroverov, V. N.; Scuseria, G. E.; Tao, J.; Perdew, J. P. *J. Chem. Phys.* **2003**, *119*, 12129−12135.

(39) Hay, P. J.; Wadt, W. R. *J. Chem. Phys.* **1985**, *82*, 270−283.

(40) Hay, P. J.; Wadt, W. R. *J. Chem. Phys.* **1985**, *82*, 299−310.

(41) Wadt, W. R.; Hay, P. J. *J. Chem. Phys.* **1985**, *82*, 284−298.

(42) Dai, B.; Deng, K. M.; Yang, J. L.; Zhu, Q. S. *J. Chem. Phys.* **2003**, *118*, 9608−9613.

(43) Weakliem, H. A. *J. Chem. Phys.* **1962**, *36*, 2117−2140.

(44) Bosi, F.; Halenius, U.; Andreozzi, G. B.; Skogby, H.; Lucchesi, S. *Am. Mineral.* **2007**, *92*, 27−33.

(45) Taran, M. N.; Rossman, G. R. *Am. Mineral.* **2001**, *86*, 973−980.